
Figures and figure supplements

Magnesium efflux from *Drosophila* Kenyon cells is critical for normal and diet-enhanced long-term memory

Yanying Wu *et al*

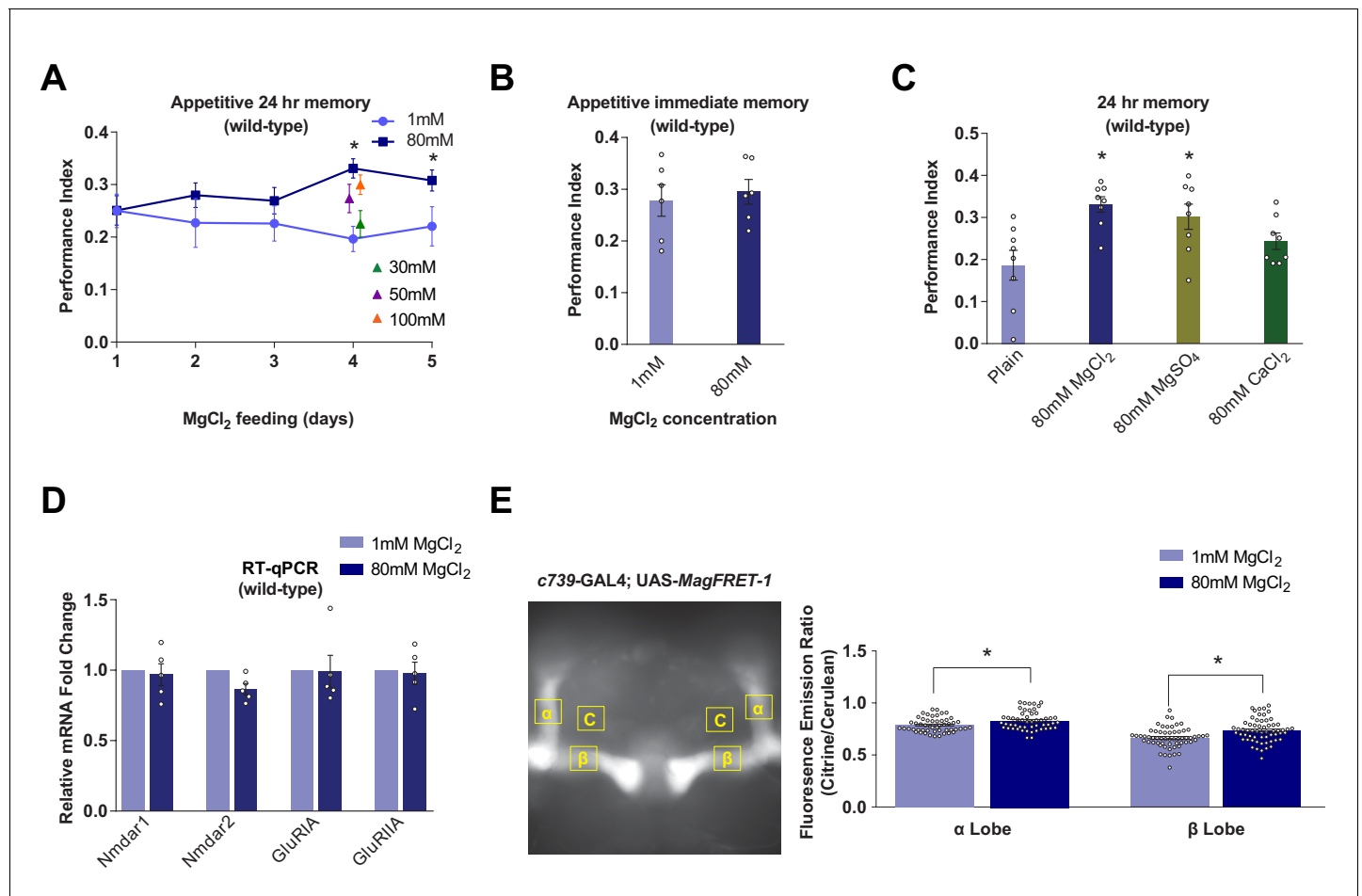


Figure 1. Dietary Mg²⁺ supplementation enhances *Drosophila* long-term memory. (A) Wild-type flies were trained and tested for 24 hr appetitive memory after 1–5 days of ad libitum feeding on food supplemented with Mg²⁺. Memory was significantly enhanced in flies fed for 4 days with 80 mM MgCl₂, as compared to those fed with 1 mM. 80 mM MgCl₂ produced marginally higher performance than 50 mM or 100 mM and so was considered optimal (asterisks denote p < 0.05, t-test between 1 mM and 80 mM groups for each time point, n = 6–8). (B) 4 days of 80 mM MgCl₂ food did not enhance immediate memory. (C) Appetitive 24 hr memory was enhanced by feeding wild-type flies for 4 days with MgCl₂ and MgSO₄, but not CaCl₂. Asterisks denote significant differences (p < 0.05, ANOVA, n = 6) between Mg²⁺ fed and plain groups. (D) RT-qPCR showed no significant differences in glutamate receptor mRNA expression between 1 mM and 80 mM fed flies (t-test, n = 5). (E) c739-GAL4; UAS-MagFRET-1 flies were fed for 4 days on food supplemented with Mg²⁺. Brains were dissected and fixed and a fluorescence emission ratio measurement (Citrine/Cerulean) was taken as an indicator of [Mg²⁺]. The MagFRET signal was significantly greater in the αβ lobes of flies fed with 80 mM MgCl₂ than those fed with 1 mM MgCl₂ (p < 0.05, t-test, n = 52–60). Unless otherwise noted, all data are mean ± standard error of mean (SEM). Asterisks denote significant differences (p < 0.05), individual data points displayed as open circles.

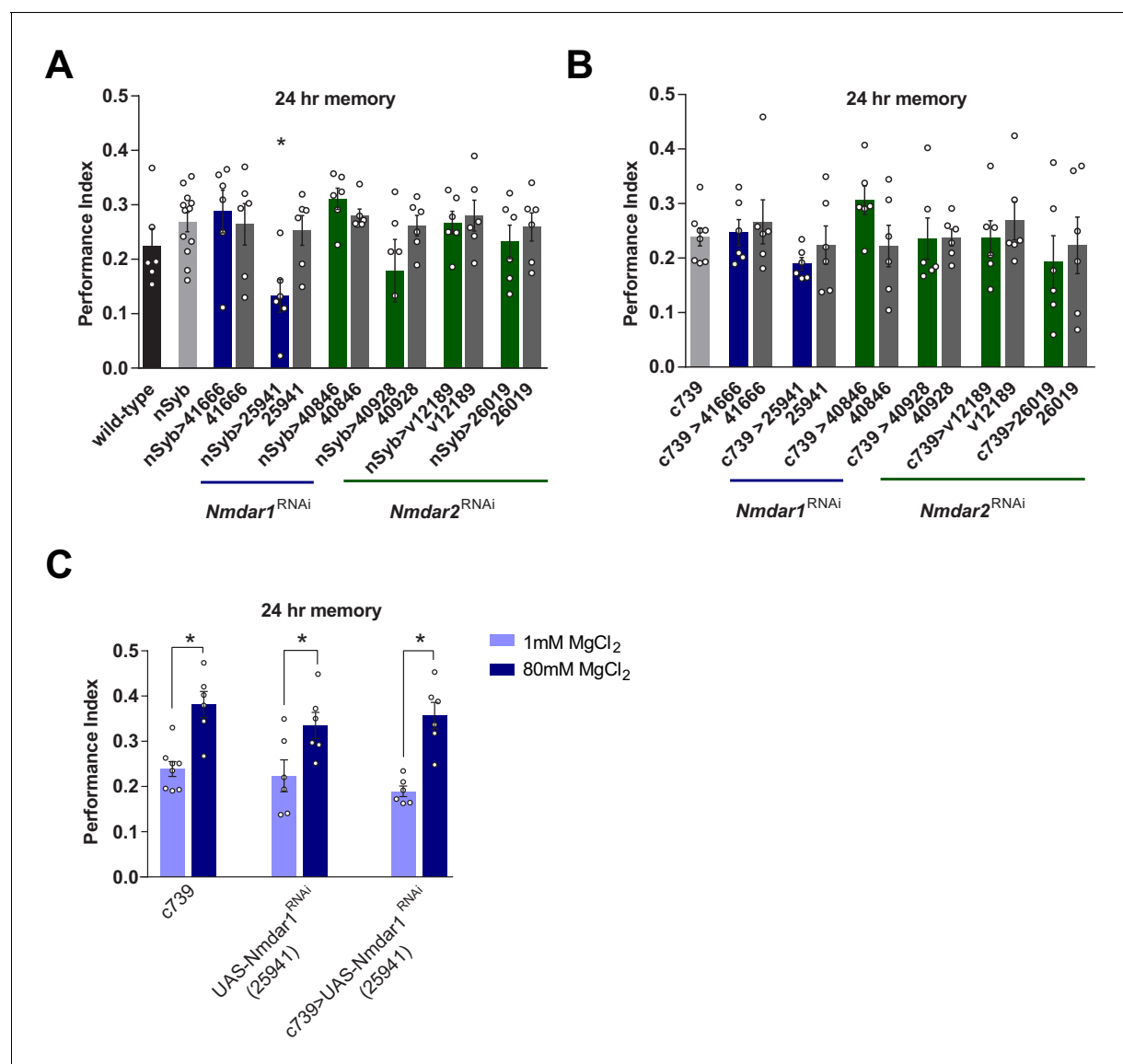


Figure 1—figure supplement 1. Knockdown of N-methyl-D-aspartate glutamate receptor (NMDAR) in mushroom bodies does not impair Mg^{2+} -enhanced memory. (A) Expressing UAS-*Nmdar1*^{RNAi} (BDSC line 25941) in all neurons with *nSyb*-GAL4 significantly impaired 24 hr memory ($p < 0.05$, ANOVA, $n = 6-12$). (B) Expressing UAS-*Nmdar1*^{RNAi} (BDSC line 25941) in $\alpha\beta$ Kenyon cells (KCs) with *c739*-GAL4 did not alter memory (ANOVA, $n = 6-8$). (F) Mg^{2+} feeding enhanced LTM in flies expressing UAS-*Nmdar1*^{RNAi} (BDSC line 25941) in $\alpha\beta$ KCs and also in controls ($p < 0.05$, t-test, $n = 6-8$). Data are mean \pm SEM. Individual data points are plotted as circles.

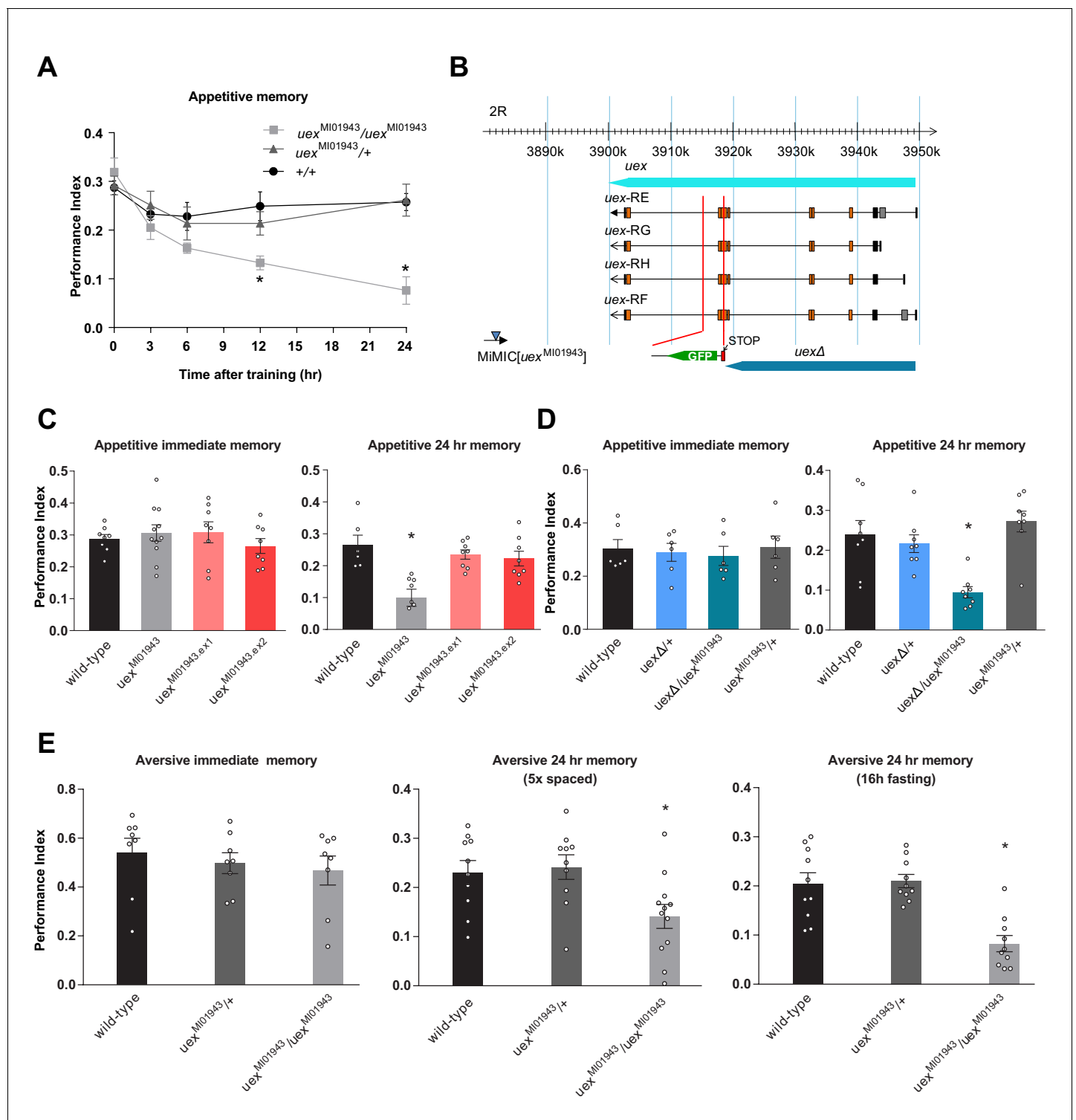


Figure 2. $uex^{MI01943}$ mutant flies have defective long-term memory (LTM). (A) Appetitive memory retention was tested at various times after training. Flies homozygous for $uex^{MI01943}$ showed a significant defect in memory from 12 hr after training, as compared to the performance of heterozygous $uex^{MI01943}/+$ and wild-type control flies ($p < 0.05$, ANOVA, $n = 6-10$). (B) The *uex* locus lies on chromosome 2R between 3,900,285 and 3,949,425 (light blue bar). The four alternate *uex* transcripts, *uex*-RE, *uex*-RG, *uex*-RH, and *uex*-RF, all encode the same protein. The $uex^{MI01943}$ MiMIC (blue triangle) resides ~17 kb downstream of the *uex* coding region. The CRISPR/Cas9 edited *uex* Δ allele replaces a 3047 bp fragment, including Exon 7 of *uex* with a STOP signal (termination codon in all three reading frames) and a GFP cassette, truncating the *uex* reading frame (dark blue bar). (C) Precise excision of the $uex^{MI01943}$ MiMIC restores normal 24 hr memory to $uex^{MI01943.ex1}$ and $uex^{MI01943.ex2}$ flies ($p < 0.05$, ANOVA, $n = 8-11$). (D) *uex* Δ fails to complement Figure 2 continued on next page

Figure 2 continued

the 24 hr memory defect of $uex^{MI01943}$ ($p < 0.05$, ANOVA, $n = 6-8$). (E) Flies homozygous for $uex^{MI01943}$ showed a significant defect in aversive LTM, as compared to the performance of heterozygous $uex^{MI01943/+}$ and wild-type control flies ($p < 0.05$, ANOVA, $n = 8-12$). An LTM defect was also observed following five cycles of aversive spaced training and a 16 hr fasting facilitated one-cycle training protocol. Immediate aversive memory was unaffected in $uex^{MI01943}$ homozygous mutant flies.

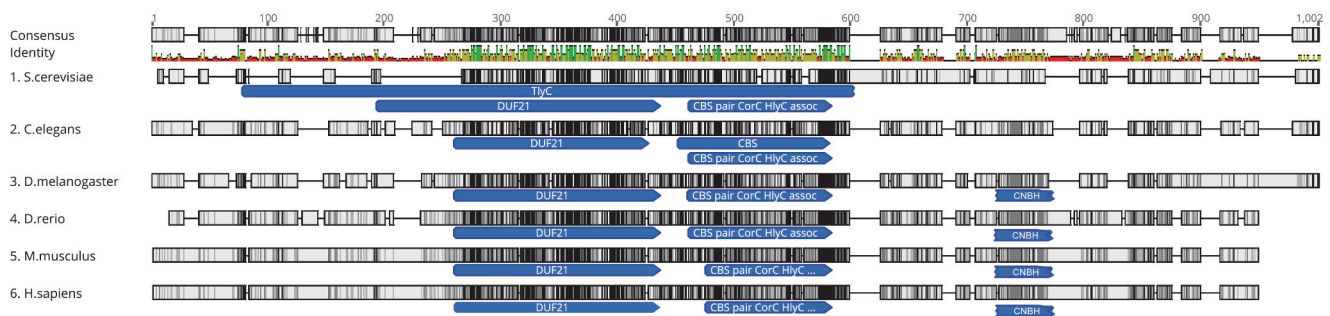
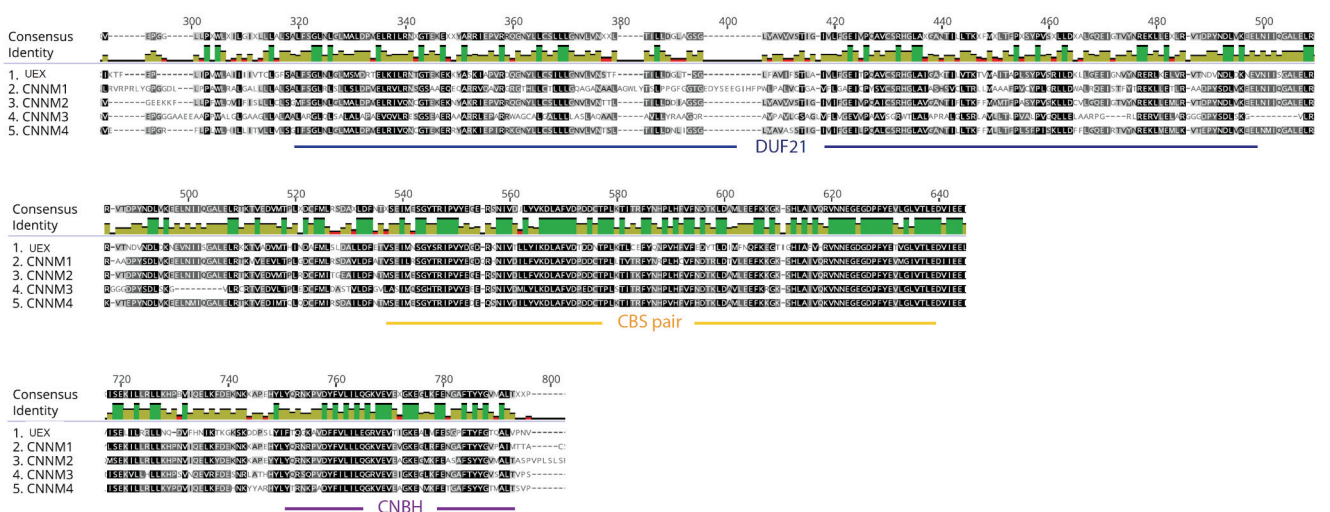
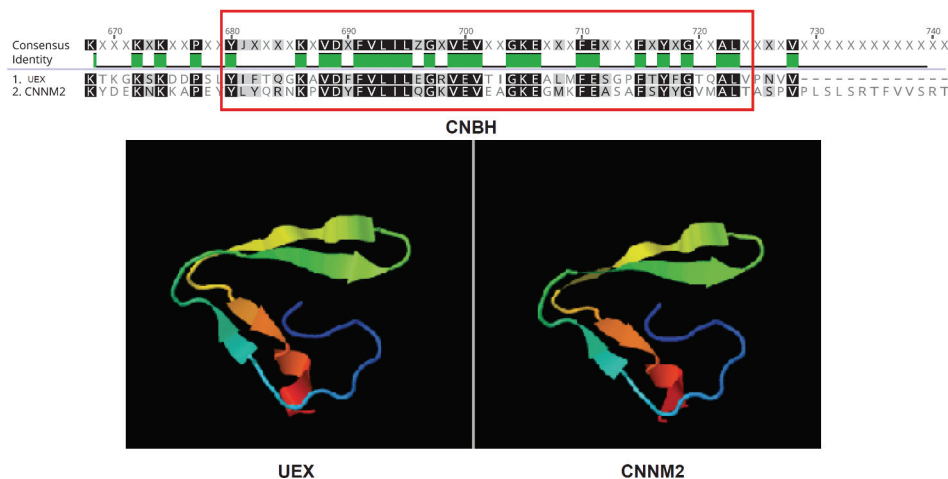
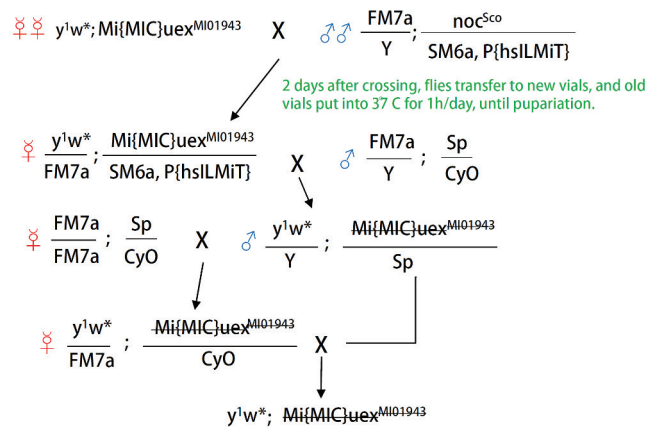
A**B****C**

Figure 2—figure supplement 1. Conservation of UEX with its orthologs. (A) Alignment of the protein sequences of UEX and its orthologs. The DUF21 and CBS pair domains are highly conserved. Accession numbers for these protein sequences are: 1.NP_014581.1 (Mam3p in *Saccharomyces cerevisiae*), 2.NP_503052.1 (CNM1 in *Caenorhabditis elegans*), 3.NP_001104391.2 (UEX in *Drosophila melanogaster*), 4.NP_001138257.1 (CNM2 in *Danio rerio*), 5.NP_001291047.2 (CNM2 in *Mus musculus*), 6.NP_00106119.3 (CNM2 in *Homo sapiens*). (B) Focus on the DUF21, CBS pair, and cyclic nucleotide-binding (CNBH) domains. (C) Structural models of UEX and CNM2. The models are color-coded by conservation, with a consensus identity bar at the top.

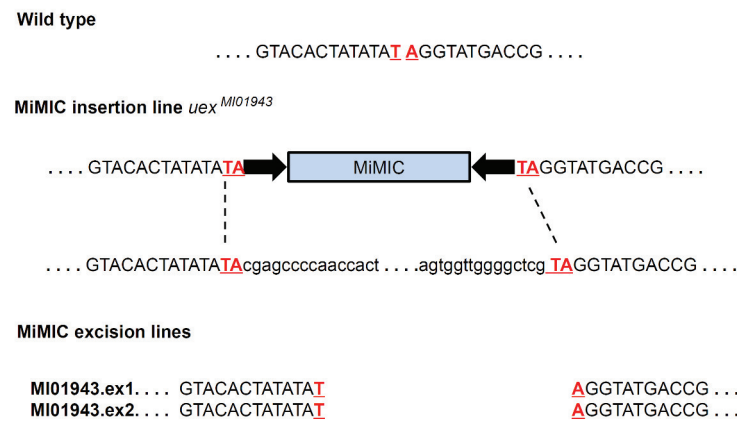
Figure 2—figure supplement 1 continued

binding homology (CNBH) domains from UEX and CNNM1-4. Similarity in each aligned sequence is proportional to its gray scale, that is, darker color corresponds to greater similarity. Accession numbers for these protein sequences are: 1.NP_001104391.2 (UEX in *Drosophila melanogaster*), 2.NP_065081.2 (CNNM1 in *Homo sapiens*), 3.NP_060119.3 (CNNM2 in *Homo sapiens*), 4.NP_060093.3 (CNNM3 in *Homo sapiens*), 5.NP_064569.3 (CNNM4 in *Homo sapiens*). (C) Protein sequence alignment of the CNBH domains (red rectangle) between UEX and CNNM2 shows high similarity (TM score = 0.98, top panel). The predicted 3D structures of the CNBH domain (lower panel) of UEX (left) and CNNM2 (right) also resemble each other.

A Mating scheme for the *Minos* excision lines:



B *Minos* excision sequence details:



C CRISPR/Cas9 editing scheme for the *uexΔ* line:

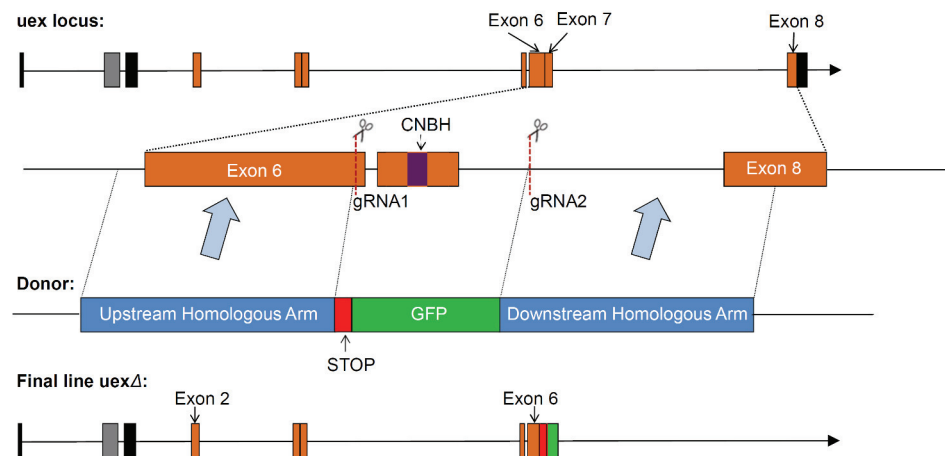


Figure 2—figure supplement 2. Construction schemes for *uex* *Minos* excision and creation of the *uexΔ* allele. (A) Mating scheme for *Minos* excision from *uex*^{MI01943} flies. (B) DNA sequence around the MiMIC insertion. Successful excision events were identified in flies with body color reverted to Figure 2—figure supplement 2 continued on next page

Figure 2—figure supplement 2 continued

yellow. Genomic DNA from progeny of these flies was extracted, and the *uex* locus was PCR amplified and sequenced. Two lines (*uex*^{MI01943.ex1} and *uex*^{MI01943.ex2}) were confirmed to be precise excision events, which restored their genomic sequence to the wild-type form. (C) CRISPR-Cas9 editing scheme for the *uexΔ* lesion. A fragment of 3047 bp spanning part of Exon 6, Exon 7, and part of Exon 8 of the *uex* locus was replaced by a STOP signal and a GFP cassette. The original sequence was cut by two gRNAs flanking Exon 7, and the new sequence was introduced by homologous recombination using a double-stranded DNA donor. The final *uexΔ* locus contains a truncated *uex* reading frame. The GFP cassette facilitates identification of flies with the edited locus.

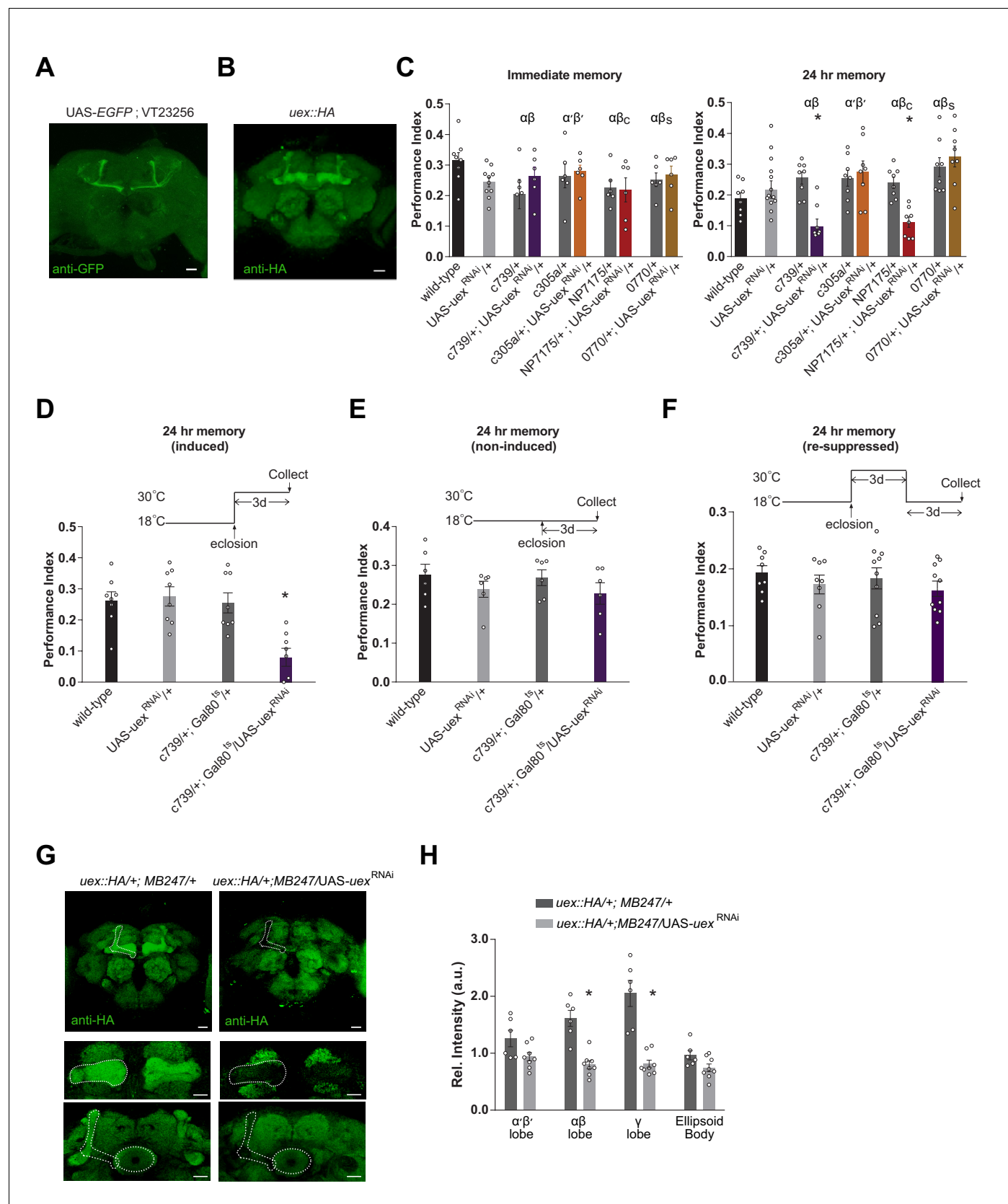


Figure 3. Knocking down *uex* expression in $\alpha\beta$ Kenyon cells (KCs) impairs LTM. (A) A *uex* promoter fragment-GAL4 directs GFP expression in $\alpha\beta$ KCs. Anti-GFP immunostained *uex*-GAL4 (VT23256); UAS-EGFP line. (B) Anti-HA immunostaining of brains harboring the CRISPR/Cas9-edited *uex::HA* locus

Figure 3 continued on next page

Figure 3 continued

shows strong labeling of UEX in all the major subdivisions of the mushroom body (MB). Scale bars 20 μm . (C) RNAi knockdown of *uex* in all $\alpha\beta$ (c739-GAL4) or just $\alpha\beta_c$ (NP7175-GAL4) KCs specifically impaired 24 hr memory. $\alpha\beta_s$ (0770-GAL4) or $\alpha'\beta'$ (c305a-GAL4) KC expression had no effect ($p < 0.05$, ANOVA, $n = 6$ –10 for immediate and $n = 8$ –14 for 24 hr memory). (D) Defective LTM was observed if *uex*^{RNAi} expression was confined to $\alpha\beta$ KCs of adult flies using GAL80^{ts}-mediated temporal control. (E) LTM performance was unaffected if the *uex*^{RNAi} was kept suppressed throughout and (F) LTM performance was restored to normal levels if expression of *uex*^{RNAi} was re-suppressed for 3 days ($p < 0.05$, ANOVA, $n = 6$ for immediate and $n = 8$ for 24 hr memory). (G) Immunostaining shows the effectiveness of *uex*^{RNAi}. Fluorescence intensity in the $\alpha\beta$ and γ lobes of *uex::HA* flies decreased significantly when UAS-*uex*^{RNAi} was expressed with MB247-GAL4. Scale bars 20 μm . (H) Quantification of fluorescence intensity in G ($p < 0.05$, t-test, $n = 6$ –8).

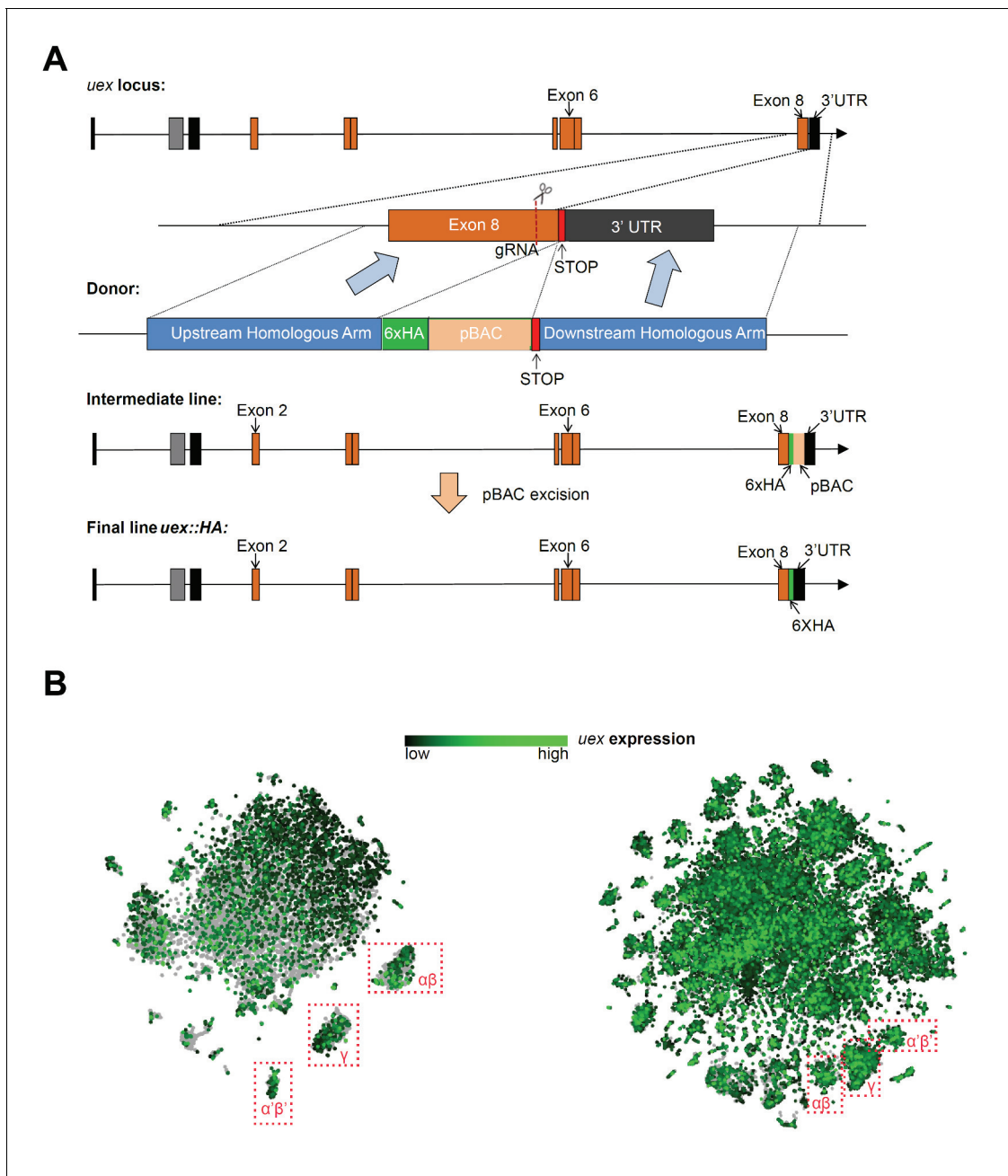


Figure 3—figure supplement 1. Construction scheme for the *uex::HA* line and tSNE plots of *uex* expression. (A) CRISPR-Cas9 editing scheme for production of the *uex::HA* locus. A 6xHA tag was inserted immediately before the STOP codon of *uex* using the 2-step ScarlessDsRed system. In step 1, a pBAC transposon containing a DsRed cassette and a 6xHA tag was inserted in frame with the *uex* ORF, just prior to the STOP codon, through homologous recombination. In step 2, the pBAC transposon was excised to leave only the 6xHA tag in the final *uex::HA* locus. (B) tSNE plots show the broad expression of *uex* in the fly brain, which is consistent with the *uex::HA* staining result in **Figure 3B**. Left, data from **Croset et al., 2018** and right from **Davie et al., 2018** were plotted using the online Scope viewer (<http://scope.aertslab.org>).

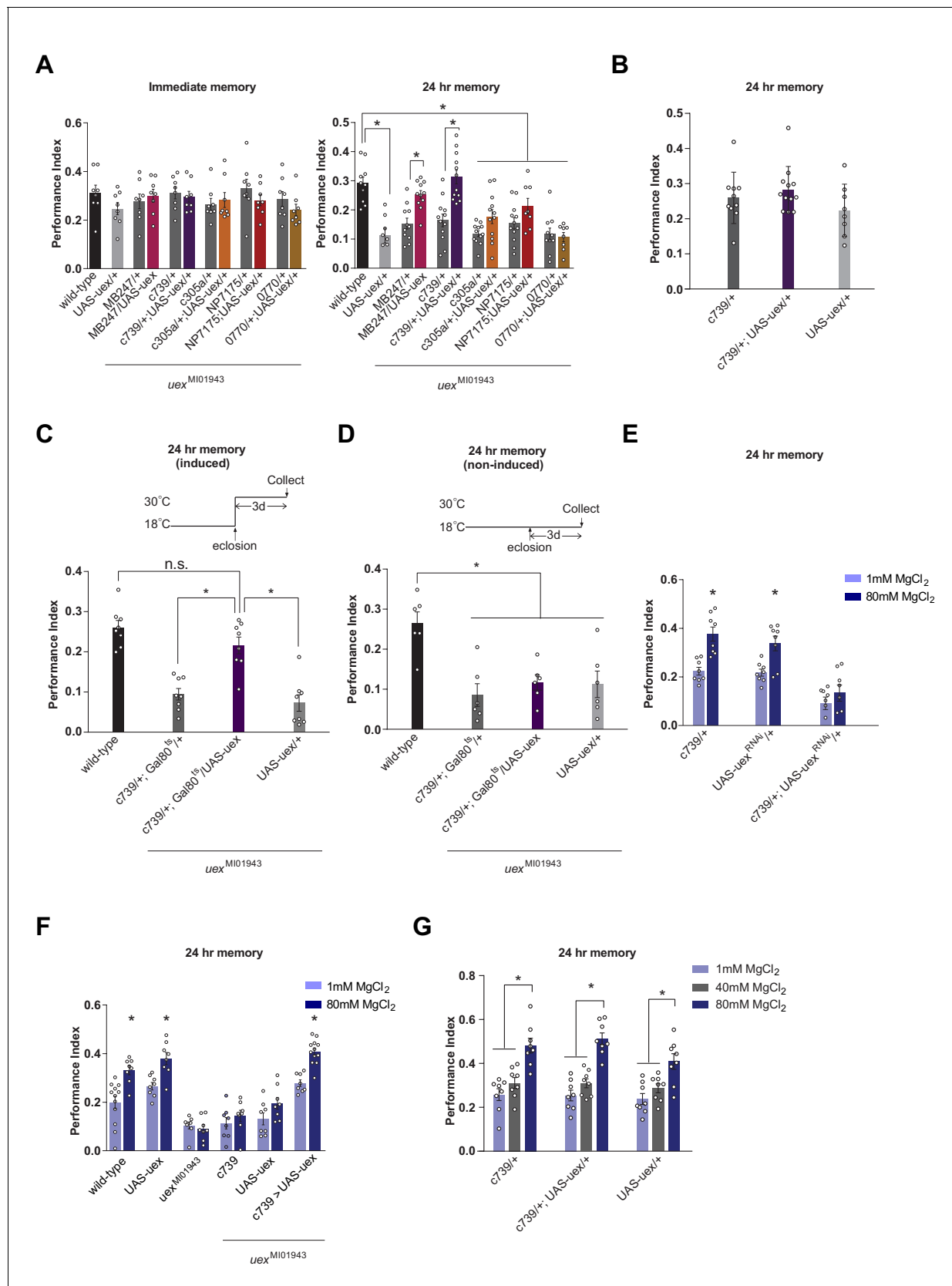


Figure 4. Rescue of the LTM defect in *uex^{MI01943}* flies. Restoring expression of UAS-*uex* in $\alpha\beta$ and γ (MB247-GAL4) or $\alpha\beta$ Kenyon cells (KCs) rescued 24 hr memory performance of *uex^{MI01943}* flies, whereas expression in $\alpha\beta_c$, $\alpha\beta_s$ or $\alpha'\beta'$ KCs did not (p < 0.05, ANOVA and t-test, n = 8–12). (B)

Figure 4 continued on next page

Figure 4 continued

Overexpression of UAS-*uex* in $\alpha\beta$ KCs did not enhance 24 hr memory performance in wild-type flies (ANOVA, $n = 8-12$). (C) Defective LTM was rescued if UAS-*uex* expression was confined to $\alpha\beta$ KCs of adult flies using GAL80^{ts} mediated temporal control ($p < 0.05$, ANOVA, $n = 6$ for immediate and $n = 8$ for 24 hr memory) but (D) remained defective if UAS-*uex* expression was not released. (E) Memory enhancement with dietary Mg^{2+} is supported by UEX in $\alpha\beta$ KCs. Memory of flies expressing UAS-*uex*^{RNAi} in the $\alpha\beta$ KCs cannot be enhanced with Mg^{2+} feeding (t-test, $n = 8$). (F) Memory of *uex*^{M101943} mutant flies cannot be enhanced with Mg^{2+} feeding, but enhancement was restored by expressing UAS-*uex* in $\alpha\beta$ KCs ($p < 0.05$, t-test, $n = 8-12$). (G) Memory of wild-type flies was not sensitized to Mg^{2+} enhancement by overexpressing UAS-*uex* in $\alpha\beta$ KCs. Memory was enhanced if the flies were fed with 80 mM $MgCl_2$, but not with suboptimal 40 mM $MgCl_2$ ($p < 0.05$, ANOVA, $n = 8$).

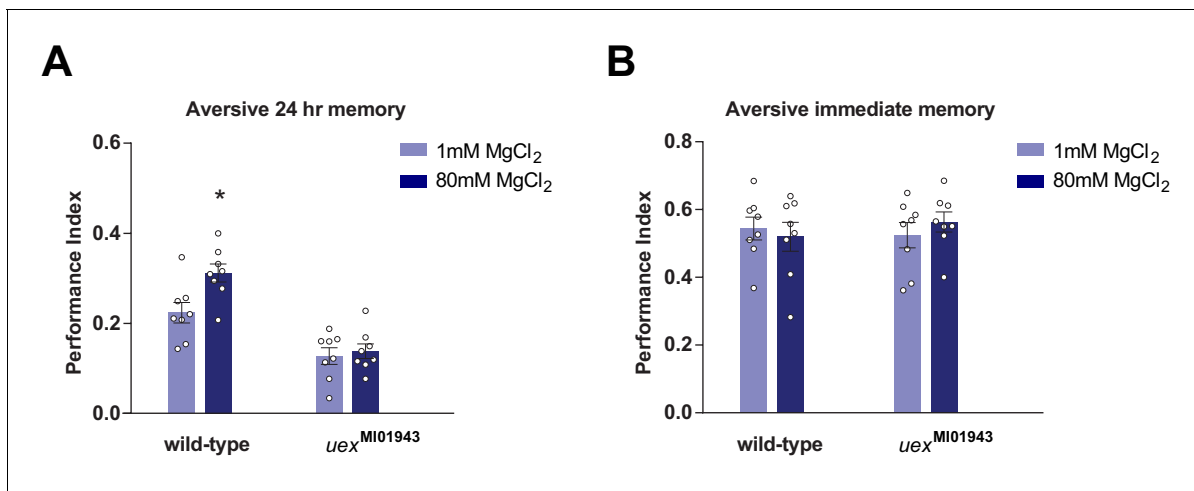


Figure 4—figure supplement 1. Mg²⁺ feeding enhanced LTM after aversive spaced training in wild-type but not *uex*^{MI01943} mutant flies. (A) 24 hr memory after five spaced trials of aversive training was enhanced in wild-type, but not *uex*^{MI01943} mutant flies, fed for 4 days beforehand with MgCl₂ ($p < 0.05$, t-test, $n = 8$). (B) 4 days of 80 mM MgCl₂ food did not enhance immediate aversive memory in either wild-type or mutant flies (t-test, $n = 8$).

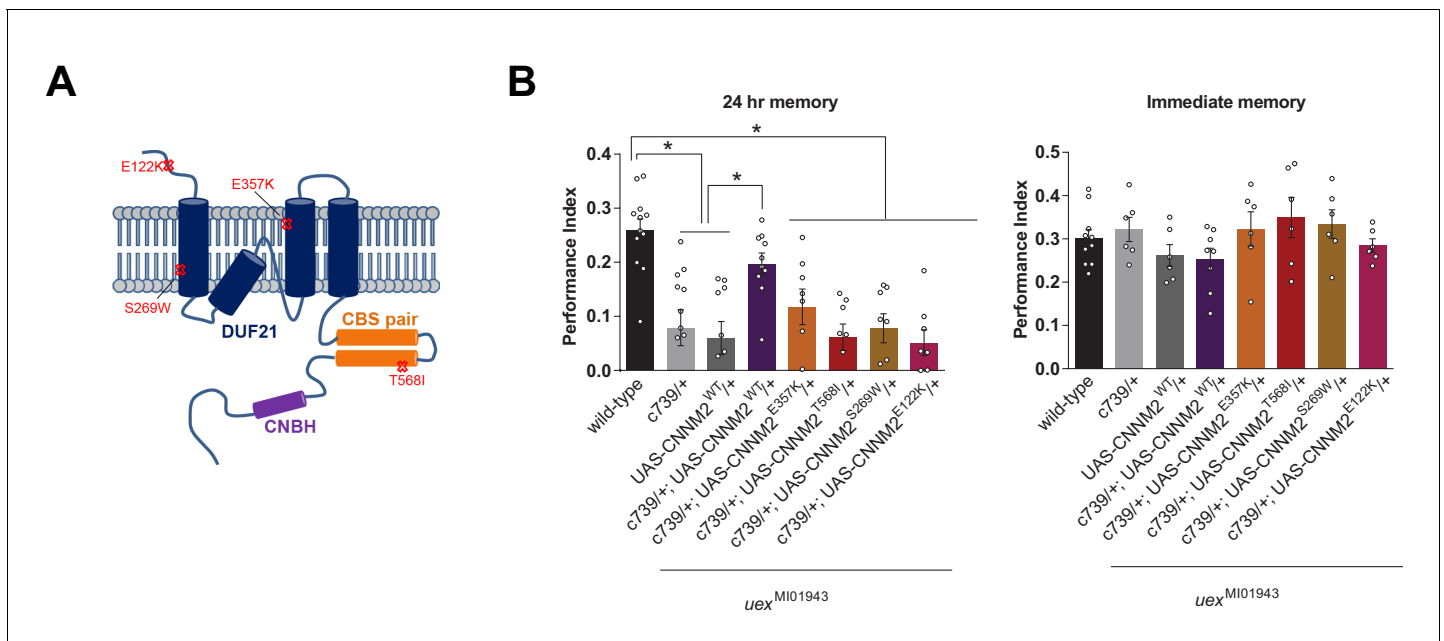


Figure 5. *uex* encodes an evolutionarily conserved Mg^{2+} transporter. **(A)** Model of CNNM2 protein structure showing clinically relevant point mutations. Adapted and modified from *Arjona et al., 2014*. **(B)** Overexpression of wild-type, but not mutant, CNNM2 in $\alpha\beta$ Kenyon cells rescues the memory defect of *uex*^{M101943} mutant flies ($p < 0.05$, ANOVA, $n = 6-8$ for immediate and $n = 8-12$ for 24 hr memory).

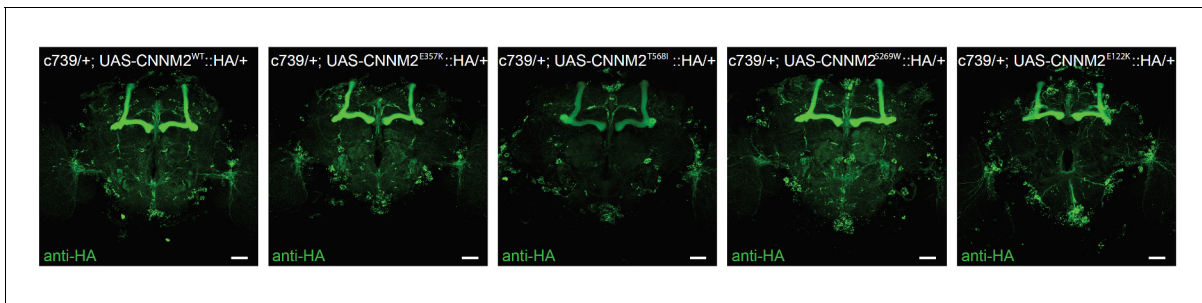


Figure 5—figure supplement 1. Transgenic expression of mutant variants of CNNM2. Anti-HA immunostained brains from flies expressing UAS-CNNM2::HA variants driven by c739-GAL4. Genotype from left to right: c739/+; UAS-CNNM2^{WT}::HA/+, c739/+; UAS-CNNM2^{E357K}::HA/+, c739/+; UAS-CNNM2^{T568I}::HA/+, c739/+; UAS-CNNM2^{S269W}::HA/+, c739/+; UAS-CNNM2^{E122K}::HA/+. Scale bar 20 μm.

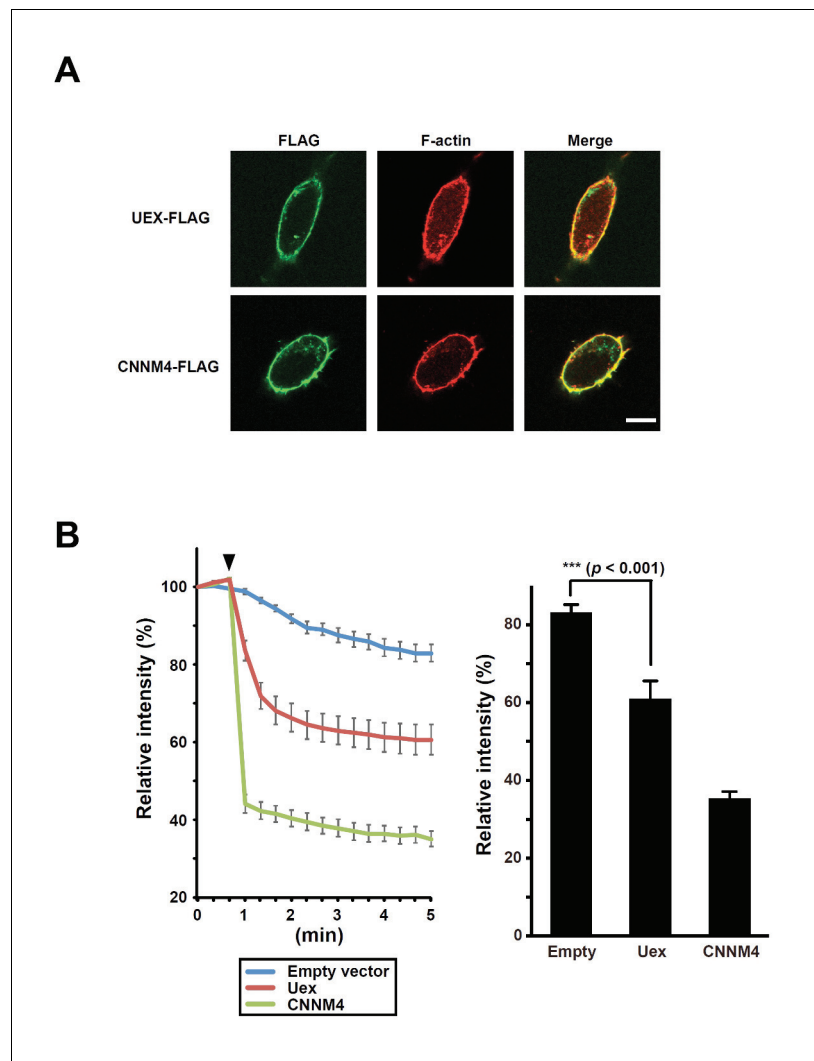


Figure 5—figure supplement 2. UEX-dependent Mg^{2+} efflux in HEK293 cells. (A) HEK293 cells transfected with *uex*-FLAG or *CNNM4*-FLAG constructs stained with anti-FLAG antibody (green) and rhodamine-phalloidin (red). Scale bar 10 μm . (B) Mg^{2+} -efflux assay. HEK293 cells transfected with the indicated constructs were loaded with Mg^{2+} and Magnesium Green, and subjected to Mg^{2+} -depletion at the indicated time point (arrowhead). Line plot indicates the time course of mean relative fluorescence intensities, and bar graph indicates the mean relative fluorescence intensities at 5 min. Data are mean \pm SEM (** $p < 0.001$, ANOVA, $n = 10$).

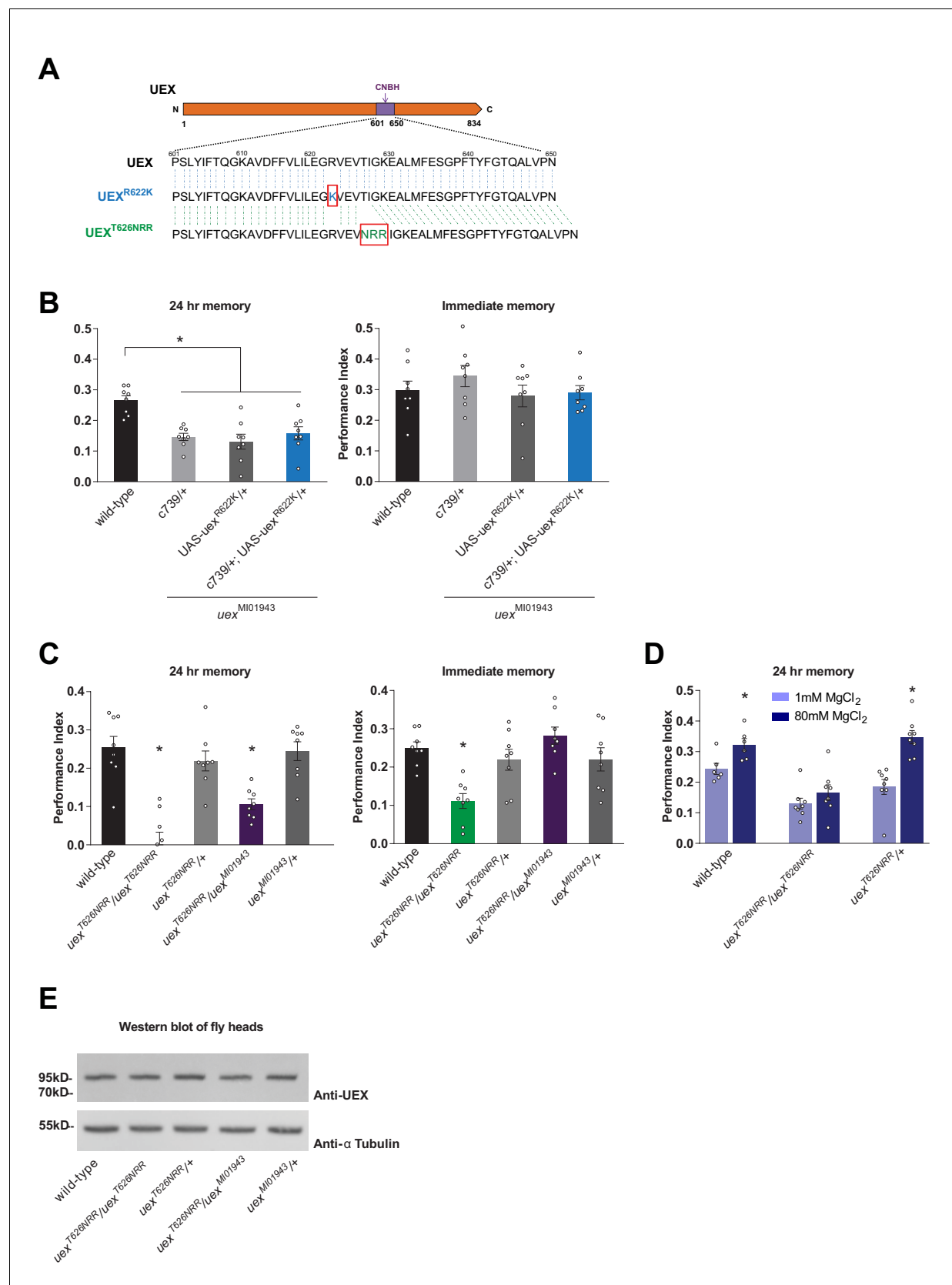


Figure 6. The cyclic nucleotide-binding homology (CNBH) domain of UEX is required for memory. (A) Schematic showing sequence detail of the CNBH domain in UEX, and the amino acid changes made in *uex*^{R622K} and *uex*^{T626NRR}. (B) Expressing a UAS-*uex*^{R622K} transgene in $\alpha\beta$ Kenyon cells did not

Figure 6 continued on next page

Figure 6 continued

rescue the LTM defect of $uex^{MI01943}$ mutant flies ($p < 0.05$, ANOVA, $n = 8$). Immediate memory was also unaffected. (C) Flies homozygous for $uex^{T626NRR}$ have defective short- and long-term memory, while trans-heterozygous $uex^{T626NRR}/uex^{MI01943}$ flies only exhibit impaired LTM ($*p < 0.05$, ANOVA, $n = 8$). (D) Dietary Mg^{2+} did not enhance memory of homozygous $uex^{T626NRR}/uex^{T626NRR}$ flies ($p < 0.05$, t-test, $n = 8$). (E) Western blot analysis of UEX protein expression in fly head extracts. Genotype from left to right: wild-type, $uex^{T626NRR}/uex^{T626NRR}$, $uex^{T626NRR}/+$, $uex^{T626NRR}/uex^{MI01943}$, $uex^{MI01943}/+$. The blot was first probed with anti-UEX antibody (upper panel), and then stripped and re-probed with anti-Tubulin antibody (lower panel) as a loading control.

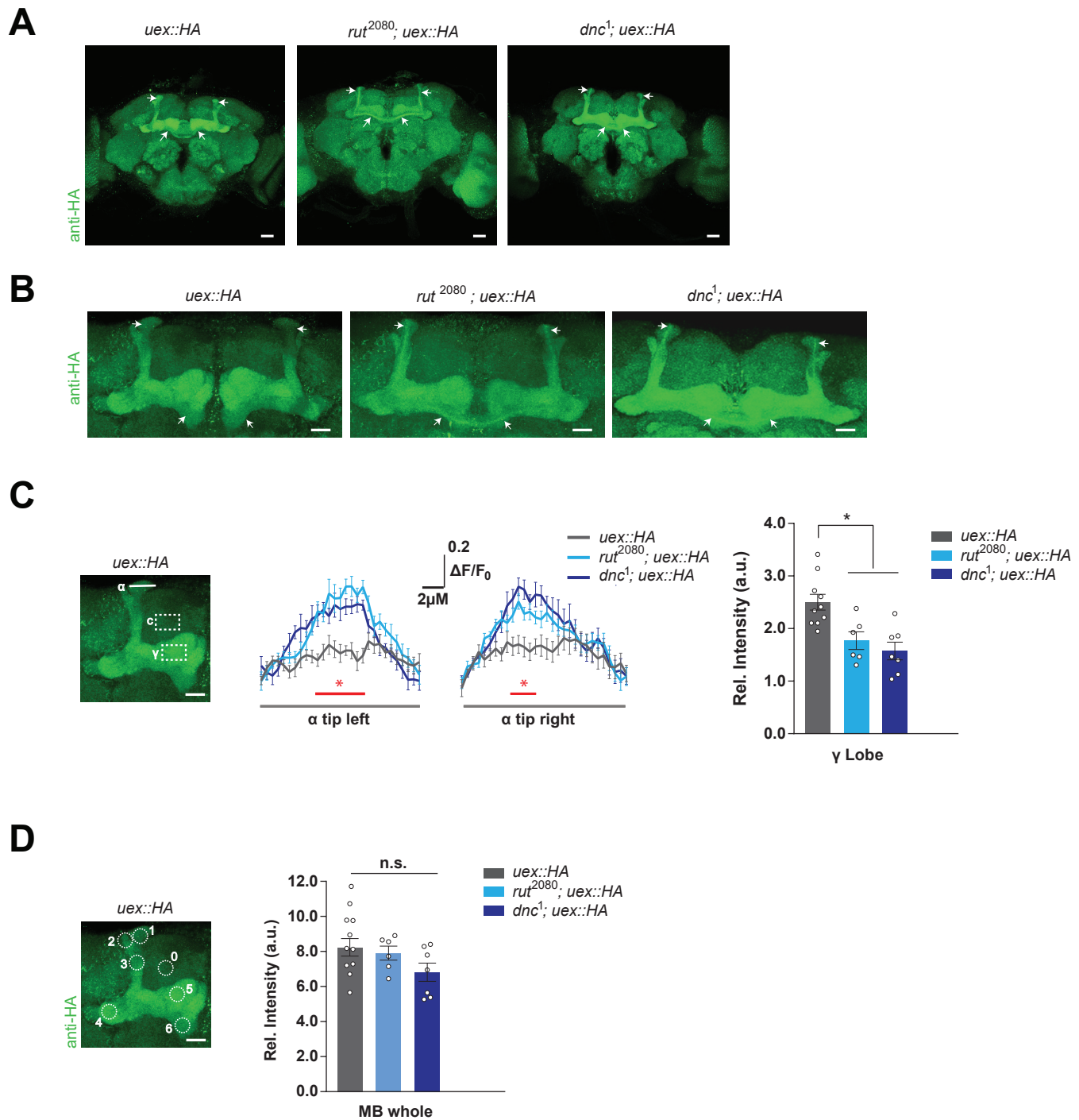


Figure 7. Kenyon cell (KC) *uex* expression is altered in *rutabaga* and *dunce* mutant flies. (A) Anti-HA stained brains reveal UEX::HA protein localization is altered in *rut²⁰⁸⁰; uex::HA* and *dnc¹; uex::HA* flies, becoming more prominent in $\alpha\beta_c$ KCs (arrows). Scale bars 20 μm . (B) Enlarged images of the mushroom bodies (MBs) highlighting $\alpha\beta_c$ KC expression in *rut²⁰⁸⁰* and *dnc¹* mutant flies, as compared with wild-type *uex::HA* flies. Scale bars 20 μm . (C) Quantification of fluorescence intensity. Left, micrograph with a measurement line through the α lobe tip and rectangular ROIs for the γ lobe and a control area. Middle, relative fluorescence intensity profiles across the α lobe tip show significantly higher signal in *rut²⁰⁸⁰* and *dnc¹* mutant flies in the center region occupied by the $\alpha\beta_c$ core KCs (* $p < 0.05$, ANOVA, $n = 6-10$). Right, the relative intensity in the γ lobe was significantly lower in *rut²⁰⁸⁰* and *dnc¹* mutant flies, as compared to wild-type controls (* $p < 0.05$, ANOVA, $n = 6-10$). Scale bars 10 μm . (D) Left, micrograph showing circular ROIs. Right, Figure 7 continued on next page

Figure 7 continued

quantification. Total intensity over all six ROIs on the MBs was not significantly different between the *rut*²⁰⁸⁰, *dnc*¹ and wild-type brains ($p > 0.13$; ANOVA, $n = 6-10$).

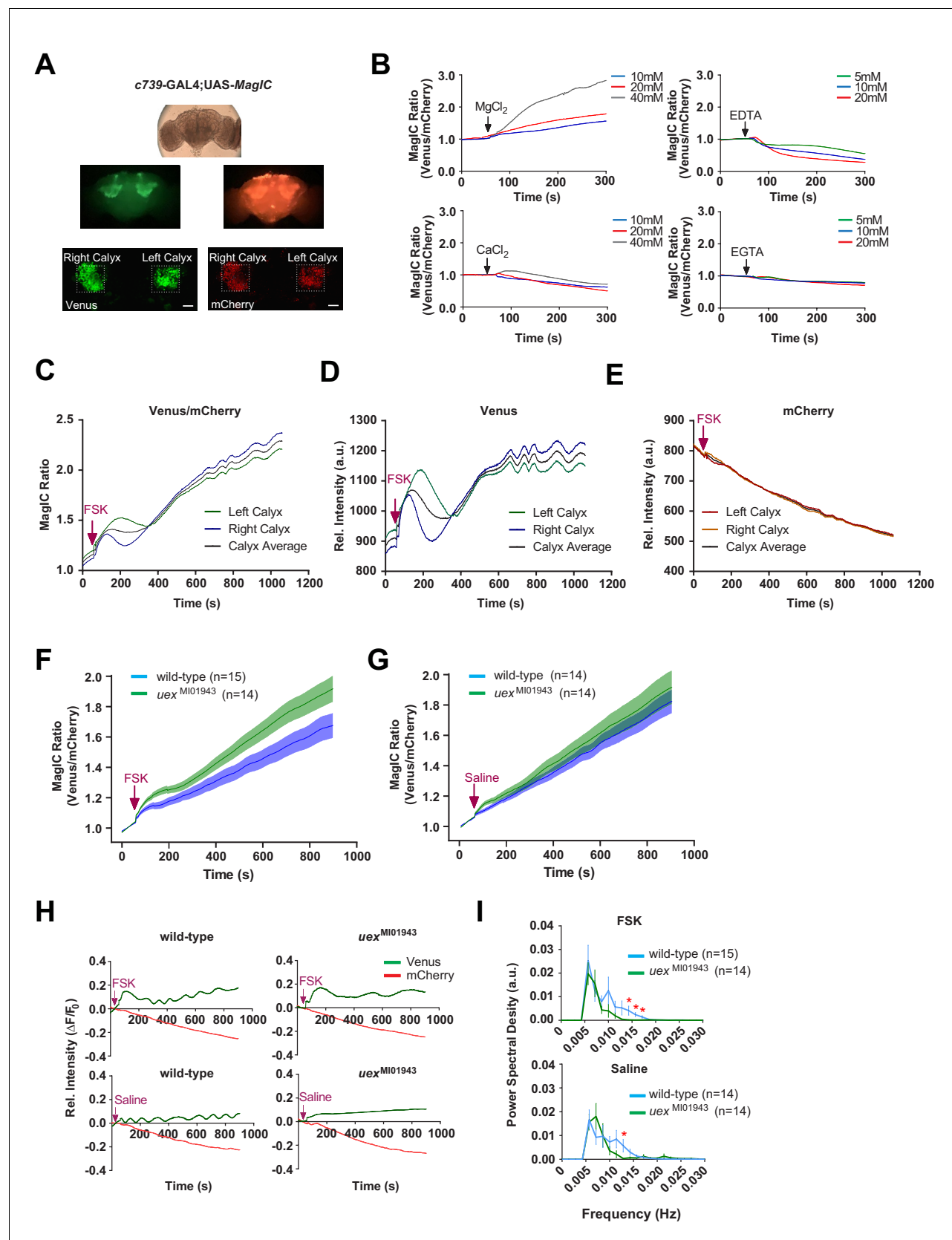


Figure 8. UEX limits a rise in $[Mg^{2+}]_i$ and supports a slow oscillation in $\alpha\beta$ Kenyon cells (KCs). (A) Explant fly brain expressing UAS-MagIC driven by *c739-GAL4*. Upper panel, wide-field phase contrast view; middle panels, fluorescence views of Venus and mCherry channels; lower panel, confocal images of Right Calyx, Left Calyx, Venus, and mCherry. Figure 8 continued on next page

Figure 8 continued

section at the level of the KC somata showing Venus and mCherry channels. Scale bars 20 μm . (B) MagIC selectively responds to changes in $[\text{Mg}^{2+}]_i$ in KCs. Traces of MagIC ratio following bath application of 10, 20, or 40 mM MgCl_2 or CaCl_2 ; 5, 10, or 20 mM EDTA or EGTA. (C) Representative trace of MagIC ratio following application of FSK shows an initial wave followed by a gradual rise and the development of a slow oscillation. (D) The primary responses result from changes in the Mg^{2+} -sensitive Venus signal. (E) The mCherry signal exhibits a steady decay. (F) FSK-evoked MagIC responses are greater in *uex* mutant flies. Averaged MagIC responses show that FSK induced a significantly greater increase in *uex*^{M101943} mutant than in wild-type flies. (G). Averaged saline-evoked MagIC responses were not significantly altered in *uex* mutant flies. (H) Individual Venus (green) and mCherry (red) channel traces showing that the slow oscillation is only evident in the Venus channel of wild-type, but not *uex* mutant, flies. (I) Power spectral density (PSD) analysis of the time series from 200 to 900 s of all data shows that traces from wild-type flies have significantly more oscillatory activity, centered around 0.015 Hz, than those from *uex* mutant flies.

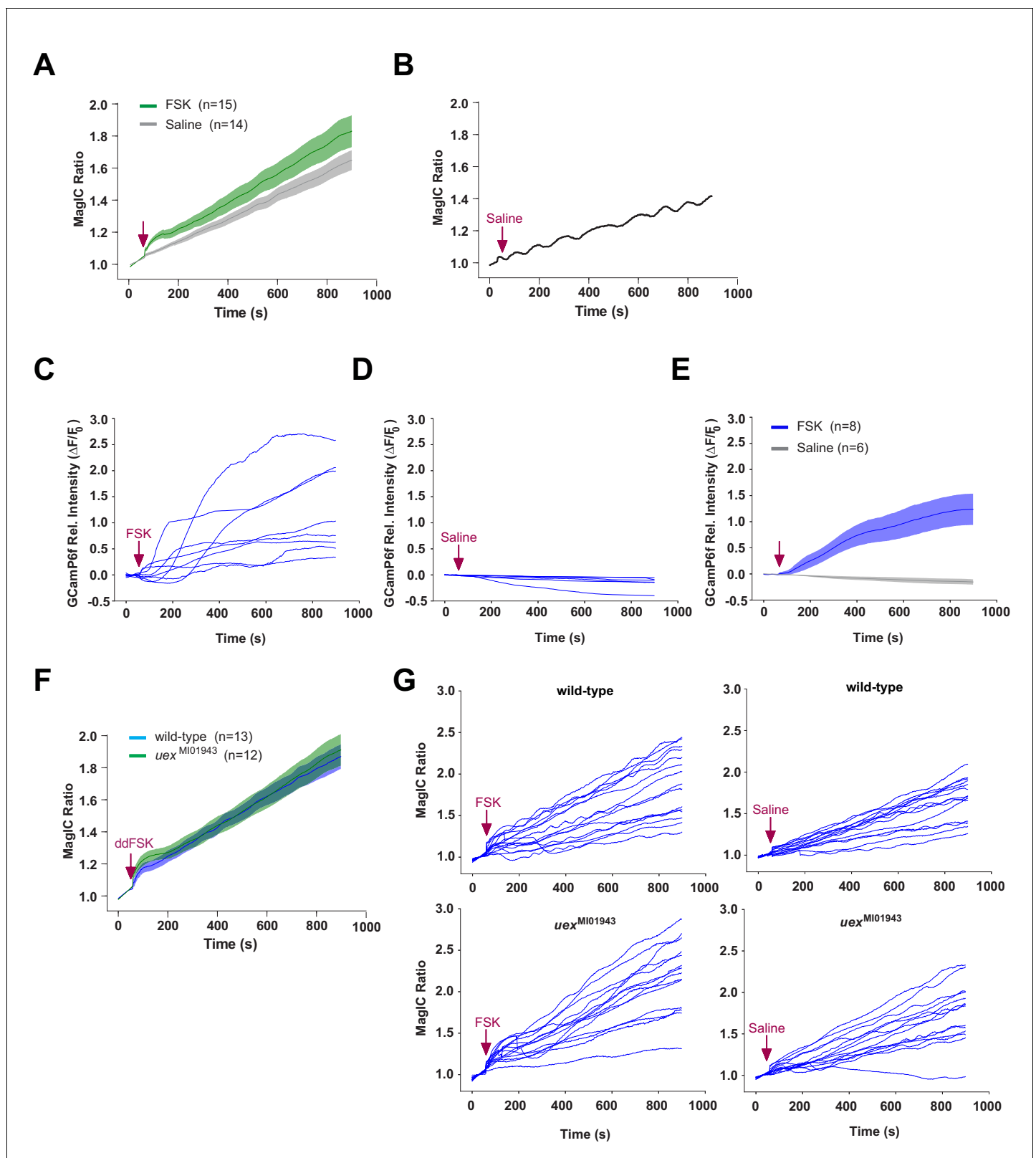


Figure 8—figure supplement 1. Individual traces for MagIC and GCaMP imaging. (A) Application of 30 μ M FSK induced a MagIC ratio response than saline application in wild-type flies (*c739/+*; *UAS-MagIC/+*). (B) A sample trace from (A) showing a fluctuating signal following saline application. (C–E) Traces of relative intensity ($\Delta F/F_0$) of GCaMP6f signal from *c739/+*; *UAS-GCaMP6f/+* flies. Slow oscillations were not observed. (C) Individual GCaMP6f

Figure 8—figure supplement 1 continued on next page

Figure 8—figure supplement 1 continued

traces following FSK application. (D) Individual GCaMP6f traces following saline application. (E) Average GCaMP6f response following FSK application is significantly stronger than that after saline. (F) The average MagIC ratio response following ddFSK application is not sensitive to *uex* mutation. Responses of wild-type (*c739/+*; UAS-MagIC/+) and *uex* mutant flies (*c739, uex^{MI01943}/uex^{MI01943}*; UAS-MagIC/+) are indistinguishable. (G) Individual MagIC ratio traces from wild-type (*c739/+*; UAS-MagIC/+ , upper panels) and *uex* mutant (*c739, uex^{MI01943}/uex^{MI01943}* , lower panels) flies following 30 μ M FSK (left panels) or saline (right panels) application.